The copper resistome of group B *Streptococcus* reveals insight into the genetic basis of cellular survival during metal ion stress

Kelvin G. K. Goh[1,2], Matthew J. Sullivan[1,2]*, and Glen C. Ulett[1,2,]*

[1]School of Pharmacy and Medical Sciences, Griffith University, Gold Coast, Queensland, Australia 4222

[2]Menzies Health Institute Queensland, Griffith University, Gold Coast, Queensland, Australia 4222

*Correspondence: Professor Glen C. Ulett, School of Pharmacy and Medical Sciences, and Menzies Health Institute Queensland, Griffith Health Centre, Griffith University, Gold Coast, Queensland 4222, Email: g.ulett@griffith.edu.au, T: +61 7 56780765, F: +61 7 55632236

*Co-correspondence: Dr Matthew J Sullivan, School of Pharmacy and Medical Sciences, and Menzies Health Institute Queensland, Griffith Health Centre, Griffith University, Gold Coast, Queensland 4222, Email: matthew.sullivan@griffith.edu.au, T: +61 7 56780915

Author Contributions: K. G. K., M. J. S., G. C. U. conceived and designed the research. K. G. K. G. performed the TraDIS experiments. M. J. S., K. G. K. G., G. C. U. constructed the GBS mutants, M. J. S. performed the ICP-OES and phenotypic assays. M. J. S., K. G. K. G., G. C. U. discussed the results and wrote the manuscript together. All authors reviewed and edited the manuscript.

Competing Interest Statement: All authors report no conflict of interest to declare.

Classification: Biological Sciences; Microbiology.

Keywords: metal ions, *Streptococcus*, copper, bacterial pathogenesis.

Abstract

In bacteria, copper (Cu) can support metabolic processes as an enzymatic cofactor but can also cause cell damage if present in excess, leading to intoxication. In group B *Streptococcus* (GBS) a system for control of Cu efflux based on the prototypical *cop* operon supports survival during Cu stress. In some other bacteria, genetic systems additional to the *cop* operon are engaged during Cu stress and also contribute to the management of cellular Cu homeostasis. Here, we examined genetic systems beyond the *cop* operon in GBS for regions that contribute to survival of GBS in Cu stress using a forward genetic screen and probe of the entire bacterial genome. A high-density mutant library, generated using pGh9-IS*S1*, was used to expose GBS to Cu stress and compared to non-exposed controls *en masse*. Nine genes were identified as essential for GBS survival in Cu stress, whereas five genes constrained GBS growth in Cu stress. The genes encode varied factors including enzymes for metabolism, cell wall synthesis, transporters and cell signalling factors. Targeted mutation of the genes validated their roles in GBS resistance to Cu stress. Excepting *copA*, the genes identified are new to the area of bacterial metal ion intoxication. We conclude that a discrete and limited suite of genes beyond the *cop* operon in GBS contribute to a repertoire of mechanisms used to survive Cu stress *in vitro* and achieve cellular homeostasis.

Significance Statement

Genetic systems for copper (Cu) homeostasis in bacteria, including Streptococci, are vital to survive metal ion stress. Genetic systems that underpin survival of GBS during Cu stress, beyond for the archetypal *cop* operon for Cu management, are undefined. We show that *Streptococcus* resists Cu intoxication by utilizing a discrete and limited suite of genes beyond the *cop* operon, including several genes that are new to the area of bacterial cell metal ion homeostasis. The Cu resistome of GBS defined here enhances our understanding of metal ion homeostasis in GBS.

Introduction

In prokaryotic and eukaryotic cells, copper (Cu) is an important cofactor for metalloenzymes (1), but when in excess, Cu can be cytotoxic. In bacteria, Cu intoxication can reflect enzyme inactivation, perturbation of metabolism, and/or redox stress, including a higher potential to generate reactive oxygen species (2). In the context of an infected host, phagocytes such as macrophages and neutrophils can mobilise intracellular pools of Cu to pro-actively expose internalized bacteria to excess metal to achieve conditions that are antimicrobial (3, 4). Such subcellular areas within infected phagocytes in which concentrated Cu exerts antimicrobial effects have been described for several bacterial pathogens (5, 6). The antimicrobial properties of Cu are thus of interest to the field of infection and immunity since these offer potential avenues for antimicrobial benefit, which might be harnessed to better control bacterial infection (4, 7, 8).

The prototypical system for Cu efflux in bacteria utilizes the *cop* operon, encompassing *copA* that encodes an ATPase efflux pump that extrudes cellular Cu ions, alongside a Cu-specific transcriptional regulator *copY*, that represses the operon (9-11). Adaptation to metal excess and limitation in bacteria is nonetheless complex. Several systems additional to the *cop* operon based on efflux proteins, including P-type ATPases are also described, and these contribute to bacterial resistance to metal stress for several pathogens, as reviewed elsewhere (5). *Streptococcus agalactiae*, also known as group B

Streptococcus (GBS) is an opportunistic bacterial pathogen of humans and animals for which a discrete genetic system for cellular management of Cu homeostasis based on the *cop* operon was recently described (12). The GBS *cop* operon regulates cellular Cu content by responding to excess Cu and de-repressing *copA* via CopY to drive Cu export from the cell (12). A functional system for Cu efflux in GBS was also shown to contribute to virulence of the bacteria during acute infection (12).

Here, we sought to identify genetic systems in addition to the *cop* operon that aid Cu management in GBS. We used a genome-wide approach based on Transposon Directed Insertion Site Sequencing (TraDIS) to probe the GBS genome for regions that support cell survival of Cu stress.

Results

Determination of growth conditions and Cu concentration required for TraDIS

To probe the entire GBS genome for regions that support the survival of this organism during Cu stress, we first evaluated the conditions for *in vitro* exposure of GBS to Cu stress, which would be suitable for a subsequent forward genetic screen. To do this, we tested a Cu concentration of 1.5 mM in Todd-Hewitt Broth (THB) medium for inhibition of GBS growth because this was sufficient to inhibit a GBS mutant deficient in *copA* (encoding a Cu efflux P-type ATPase) in a prior study (12). Growth assays verified that 1.5 mM Cu in THB was insufficient to inhibit the growth of wild-type GBS 874391 but sufficient to completely inhibit the growth of a GBS Δ*copA* mutant (Fig.1). The level of 1.5 mM Cu in THB was therefore accepted as suitable to probe for additional genes that contribute to resistance to Cu stress, as this would inhibit growth of mutants sensitive to Cu.

Identification of genes associated with Cu resistance in GBS 874391

To facilitate an extensive genome wide screen of genes required for Cu resistance in GBS 874391, we first generated a library of approximately 480,000 random IS*S1*-insertional mutants using pGh9-IS*S1*. Next, we subjected the mutant library to the growth conditions established above to identify genes associated with Cu resistance. In this assay, ~1.9 x 10^8 cells (equating to approximately 400 cells per unique mutation) from the library were inoculated in triplicate into 100ml of THB either supplemented with 1.5 mM Cu (test pool) or

116 THB without Cu supplementation (control pool), and incubated for 12 h at 37°C.
117 These conditions were chosen to permit the growth of mutants unaffected by Cu,
118 but inhibit growth of mutants sensitive to Cu (such as for Δ*copA* above). Genomic
119 DNA was extracted from each replicate and sequenced with a multiplex TraDIS
120 approach (Fig. 2A). The control pool yielded a total of 5,163,397 IS*S1*-specific
121 reads that mapped to the 874391 genome. Further analysis of the control data
122 revealed 618,263 unique insertion sites (approximately one insertion site every
123 four bp) distributed across the entire chromosome (Supplementary Fig. S1),
124 highlighting the high degree of saturation and coverage of our library.
125
126 As mutants with insertions in genes required for Cu resistance would be lost and
127 underrepresented, we screened for a loss of insertions in the test pool as
128 compared to the control pool. Using stringent selection criteria of a $\log_2$ fold
129 change ($\log_2$FC) in read counts of ≤ -2, false discovery rate (FDR) of <0.001 and
130 P value of <0.05, we identified a hit plot of genes that contributed to GBS growth
131 in Cu stress (Fig. 2B). Here, we identified nine genes as highly significantly
132 under-represented in the dataset (Table 1). Consistent with previous reports of a
133 requirement for *copA* in resisting Cu stress, *copA* was significantly under-
134 represented (~16-fold down) during Cu stress, representing validation for the
135 TraDIS approach. Interestingly, we also identified five genes that possessed an
136 enrichment of read counts ($\log_2$FC of ≥ 2) in the test pool compared to the control
137 pool, suggesting that insertions in these genes were beneficial for growth under
138 Cu stress (Table 1). Representative insertion site mapping is shown for a

selection of loci (Fig. 3A-F). We also noted a further 28 and 15 genes were under-represented and over-represented in the dataset (log_2FC between -1 to -2 or 1 to 2; Supplementary Table S1), respectively. Interestingly, this list included two genes (*rfaB* [log_2FC = -1.24] and *plyB* [log_2FC = -1.63]) which we have found to contribute to zinc resistance (Sullivan *et al,* unpublished). Hence we chose to include these two genes in subsequent experiments as representative members of the group of 28 genes significantly under-represented in the Cu-stress pool between 2-4-fold.

Characterisation and validation of Cu sensitive mutants

To validate hits from the TraDIS screen, we generated targeted isogenic mutants of several candidate genes and phenotypically analysed these mutants for survival and growth in Cu stress. The genes included *hisMJP* (CHF17_01047, 01048 and 01049), *oafA* (CHF17_00084), *yceG* (CHF17_01646), *stp1* (CHF17_00435), *ribD* (CHF17_00876), *rfaB* (CHF17_00838), and *plyB* (CHF17_00885). Firstly, colony forming unit (CFU) assays based on the conditions used for the TraDIS screen were performed to test survival of the mutants in 1.5 mM Cu after a 12 h incubation period. In this assay, besides WT and the Δ*hisMJP* mutant, all other isogenic mutants exhibited a significant decrease (~30 to 72%) in CFU counts when grown in the presence of Cu, indicating that these mutants were sensitive to Cu (Fig. 4). Notably, we also observed a significantly lower overall bacterial counts in the Δ*plyB* and Δ*stp1*

mutants as compared to WT when grown in THB, indicating that these genes may contribute to the growth of GBS in rich media.

We further explored the Cu sensitivity of the mutants by measuring growth kinetics over 12h in THB medium with and without supplemental 1.5 mM Cu. Firstly, there was no significant difference in the growth kinetics of the mutant strains compared to WT in THB (Figure 5A), excepting the Δ*rfaB* and Δ*ribD* mutants, which were significantly attenuated, or enhanced, respectively (Figure 5B). In these comparisons, the attenuated growth kinetics of the Δ*stp1* mutant approached statistical significance (P=0.054). Next, the Δ*ribD* mutant grew to higher culture densities compared to WT during stationary phase Cu stress conditions, with final attenuance (D; 600nm) values (at 12h) significantly higher (Supplementary Fig. S2). The Δ*hisMJP* strain also exhibited significantly higher final D 600nm values (at 12h) compared to WT (Supplementary Fig. S2). In THB with Cu, the Δ*oafA,* Δ*hisMJP,* Δ*plyB,* Δ*rfaB, and* Δ*stp1* mutants exhibited attenuated growth compared to WT (Figure 5C). Finally, the Δ*hisMJP,* Δ*oafA,* Δ*yceG,* and Δ*stp1* mutants were significantly attenuated for growth during Cu stress, with lower overall absorbance, or an extended lag phase, compared to control conditions (of the same strain in THB without Cu stress). Complementation of the Δ*hisMJP*, Δ*yceG* and Δ*stp1* mutants *in trans* and subsequent growth assays showed near-complete restoration of growth in Cu stress to non-Cu stress conditions (Supplementary Fig. S3).

We and others have previously reported that culture media can affect sensitivity of streptococci to Cu (11, 12). Consequently, we measured the growth of WT GBS and each isogenic mutant in nutrient limited conditions using a minimal Chemically-Defined Medium (CDM) with and without supplemental Cu (Fig. 6A). In these assays, growth of the WT strain was unaffected by the presence of 0.5mM Cu in CDM (Fig 6A; additional Cu concentrations of 0.2mM and 1.0mM shown in Supplementary Fig. S4). Several mutants (Δ*hisMJP,* Δ*plyB*, Δ*rfaB* and Δ*stp1*) exhibited significant growth defects in CDM in the absence of Cu when compared to WT (Fig. 6B). In CDM with Cu, all mutants except Δ*ribD* exhibited significantly attenuated growth compared to WT (Fig 6C). Additionally, apart from Δ*ribD*, growth of all other mutants (Δ*hisMJP*, Δ*oafA,* Δ*yceG,* Δ*plyB*, Δ*rfaB* and Δ*stp1*) were significantly attenuated compared to control conditions of the same strain in CDM without Cu stress (Fig. 6A). Notably, the attenuated growth phenotypes of each of the mutants (excepting Δ*ribD*) due to Cu stress were more severe in CDM compared to THB. Complementation of the Δ*hisMJP,* Δ*yceG*, Δ*rfaB* and Δ*stp1* mutants *in trans* showed restoration of growth in Cu stress (Supplementary Fig. S5). Interestingly, complementation of the Δ*plyB* mutant showed further attenuation of growth when under Cu stress.

Despite numerous attempts, we were unable to generate an *oafA* plasmid construct for complementation studies. Hence, we used a chelator to further

probe the role of *oafA* in Cu tolerance. To this end, we performed growth assays in CDM (+/- Cu) with varying amounts of TPEN. Here, we found that growth of Δ*oafA* was partially restored upon addition of TPEN (Supplementary Fig. S6). Taken together, these data support the observations made using our TraDIS analyses to confirm major contributions of several novel genes to tolerance of Cu stress in streptococci.

Accumulation of intracellular Cu during Cu stress

Inductively coupled optical emission spectroscopy (ICP-OES) was used to investigate if cellular Cu content is affected in each respective isogenic mutant. Standard THB medium contains 0.2±0.08 μM Cu, reflecting trace amounts in the medium (12). Our approach to quantify intracellular Cu at mid-exponential growth phase in conditions of Cu stress that are sub-inhibitory for WT and mutants was consistent with our previous study. To this end, cultures of WT and the respective mutants were grown for 2.5 h in THB or in THB supplemented with 0.5 mM Cu. In the absence of supplemental Cu, WT GBS limited intracellular Cu content such that only 0.53±0.04 μg Cu g dry weight^{-1} were detected in cultures grown in THB consistent with prior findings (12). Growth of WT in the presence of 0.5 mM Cu resulted in a significant increase in intracellular Cu, to 11.69±3.52 μg per g dry weight (Fig. 7A). A similar pattern was observed in the different mutants, where exposure to Cu also resulted in a significant increase in intracellular Cu (Fig. 7A). Strikingly, the Δ*stp1* mutant exhibited almost twice as much intracellular Cu as compared to WT (20.89±5.85 μg Cu G dry weight^{-1}), whereas the Δ*hisMJP*, Δ*ribD*

228 and Δ*rfaB* mutants contained approximately half the intracellular Cu as compared
229 to WT (4.34±1.57, 5.89±1.68 and 6.61±0.77 µg Cu G dry weight^{-1} respectively)
230 (Fig. 7B). There was no significant alteration in the intracellular Cu content for the
231 Δ*yceG*, Δ*plyB* and Δ*oafA* mutants compared to WT. A summary of the results
232 from this study is presented in Supplementary Table S2.
233

Discussion

GBS is an opportunistic pathogen that causes a diverse range of disease aetiologies in infants and adults, including skin and soft-tissue infections, arthritis, pneumonia, meningitis, urinary tract infection, and endocarditis (13). GBS expresses several virulence factors that enable the bacteria to survive in harsh conditions, such as acid stress, oxidative stress, and during infection of a host, as reviewed elsewhere (14). Metal ion stress due to excess Cu was recently demonstrated to be antimicrobial towards GBS (12). Cu is an essential micronutrient for bacteria (15), but as excess Cu can be toxic to cells, bacteria need to regulate the amount of intracellular Cu during Cu stress. This can be achieved using three mechanisms – (i) expulsion of intracellular Cu into the extracellular milieu, (ii) sequestration of Cu by Cu binding proteins, and (iii) oxidation of Cu(I) to the less toxic form of Cu(II) (16). In this study, using a forward genetic screen based on TraDIS, we identify new GBS factors that contribute significantly to the survival and growth of this pathogen in Cu stress conditions. The key findings are that (i) GBS utilizes several genes in addition to the *cop* operon to manage Cu homeostasis during Cu stress, (ii) the GBS Cu stress resistome comprises principally nine genes that are required for GBS to resist Cu stress, including *hisMJP*, *oafA*, *yceG*, *plyB*, *rfaB* and *stp1*. These genes have not previously been linked to mechanisms of bacterial resistance to Cu stress.

As a screening approach to identify novel functions of bacterial genes, TraDIS has been used to explore GBS survival in blood, which revealed protective effects of calprotectin (17-19). TraDIS analysis in the current study identified novel functions of several genes in GBS that play a role in Cu resistance. Our approach was validated through the identification of *copA* in our TraDIS screen, which encodes an exporter known to be essential for GBS Cu resistance (12). We generated defined mutants for nine other genes (with Δ*hisMJP* generated as a single mutant). There was a broad range of putative functions associated with these genes, including cell wall biogenesis (*oafA*, *plyB*, *yceG* and *rfaB*), metabolism (*hisMJP* and *ribD*) and signal transduction (*stp1*). It is perhaps unsurprising that we saw a diverse range of phenotypes amongst the isogenic deletion mutants, depending on the phenotypic assays used. Our quantitation of viable bacteria at 12h following exposure to 1.5 mM Cu showed lower recovery of the Δ*yceG*, Δ*plyB*, Δ*rfaB* and Δ*stp1* mutants, which matches the underrepresentation of insertional mutations in these genes in our TraDIS screen in this condition at this timepoint. We also noted a reduction in CFU counts in the Δ*ribD* strain in these conditions, in contrast to the significant over-representation of insert counts in this locus in the TraDIS screen. Similarly, we observed no difference in CFU values of the Δ*hisMJP* strain comparing Cu stress to the control (no Cu stress); noting this was the most significantly underrepresented gene cluster in our TraDIS dataset. We suggest that these differences may result from differences in assay design, read-out and interpretation, rather than

reflecting confliction of biological responses of the bacteria. For example, attenuance readings may not correlate with CFU estimates due to the presence of live and dead bacteria in different growth phases, or the insertional frequency observed in TraDIS due fundamental differences in assay design. Measurements of the growth kinetics of each isogenic mutant in THB or CDM showed marked attenuation compared to WT, excepting *ribD*, based on cumulative AUC analysis of attenuance values over the 12h period. These findings also show enhanced sensitivity of the mutants to Cu in a medium-dependent manner, suggesting that nutrient availability can affect Cu sensitivity in an indirect manner and this requires further study. The exact mechanisms by which these genes facilitate resistance to Cu toxicity is yet to be elucidated.

Stp1 is a serine/threonine phosphatase and is important for regulation of its cognate kinase partner Stk1 and GBS virulence, serving as a master controller of numerous cellular processes including nucleotide metabolism, cell segregation and virulence (20, 21). The Stp1/Stk1 axis feeds into virulence regulation through direct phosphorylation and inactivation of CovR (22). We found that not only is the *stp1* mutant more sensitive to Cu stress, but it also accumulates twice as much Cu than WT in Cu stress. In GBS, mutation of *stp1* leads to alterations in phosphorylation of a number of proteins, which in turn affects gene expression (20, 23). Genes differentially expressed as a result of *stp1* mutation include several ABC transporters implicated in the uptake of amino acids and metal transport (20), including up-regulation of *hisP* (identified in this study) and down-

301 regulation of *mtsABC* encoding a putative Mn transport system that is modulated
302 by Cu or Zn stress in GBS (12, 24). Indeed, Stp1 is a Mn-dependent
303 phosphatase; free Cu may displace Mn from the protein and lead to
304 lower/abolished activity, providing circumstantial clues to explain the Cu
305 sensitivity phenotype we observed in the *stp1* mutant. For example, the
306 enhanced sensitivity of the Stp1 mutant to Cu stress may be due to abrogation of
307 manganese homeostasis and disruption of nucleotide metabolism (25, 26).
308 However, the propensity for Cu to displace Mn in free proteins, although
309 discussed elsewhere (11, 27), is not well defined. The pleiotropic nature of Stp1
310 mediated processes means that the exact mechanism underpinning the
311 contribution of Stp1 to Cu resistance in GBS remains to be determined.
312
313 HisMJP encodes a putative amino acid ABC transport system in GBS. Structural
314 modelling with Phyre2 (28) revealed that HisP shares high predicted structural
315 similarity with a ratified ABC transporter substrate binding protein of *S.*
316 *pneumoniae* bound to histidine (PDB entry 4OHN). Cu sequestration by Cu-
317 binding proteins is a mechanism bacteria employ to subvert Cu toxicity, and Cu-
318 binding sites in proteins are dominated by histidine, cysteine, and methionine
319 residues, with Cu(II) having affinity for histidine (29). GBS is a histidine auxotroph
320 and overcomes this by using two different mechanisms; by importing histidine
321 from the environment (potentially via HisMJP), or by importing peptides via
322 permeases, which are then subsequently cleaved by peptidases into single
323 amino acids (30, 31). It may be that GBS deficient in *hisMJP* lacks the ability to

import histidine, and this causes a metabolic shift that requires the bacteria to obtain this essential amino acid from alternative sources, such as from peptides present in THB. Our data supports this hypothesis; the Δ*hisMJP* mutant reaches a similar CFU and absorbance compared to the WT after 12 h of growth in THB + 1.5 mM Cu, however there is a significant lag phase, during which cells may undergo a metabolic switch. However, when the Δ*hisMJP* mutant is incubated in minimal CDM + 0.5 mM Cu, which lacks peptide supplements, growth is abrogated. Interestingly, the Δ*hisMJP* mutant possessed the least amount of total intracellular Cu when subjected Cu stress in THB, which hints at a potential Cu-import role for this putative histidine transport system; perhaps via import of Cu-histidine complexes (32) in the extracellular milieu.

We identified several genes, including *ribD, ribE, ribA and ribH*, which were significantly over-represented in the TraDIS dataset; suggesting their mutation may be of benefit to Cu tolerance. In GBS, *ribDEAH* encode a synthesis pathway for riboflavin which is required for flavin adenine dinucleotide (FAD) and flavin mononucleotide (FMN) co-factor production. Generation and analysis of an isogenic mutant in the promoter-proximal gene of the putative *ribDEAH* operon, *ribD,* showed enhanced growth of the mutant in THB compared to WT (in the absence of Cu); but no difference to WT in THB + 1.5 mM Cu or in either condition in CDM. In our present study, we could not prescribe a role for *ribD* relating to Cu stress but we do not believe our TraDIS-identification of *rib* genes serves as a false positive result. For example, insertion of the ~4.6kB pGh9:IS*S1*

element (33) in the assay would cause polar effects on the entire *rib* operon. In our Δ*ribD* mutant, we targeted 1038 bp for removal, representing an in-frame, markerless, non-polar deletion (of ~94% of *ribD*). Thus, the type of mutation we made in *ribD* in this instance is not identical to the type of mutation generated by IS*S1* insertion and TraDIS analysis. Moreover, in a prior study of *S. aureus* (34), *ribD* was found to be downregulated in response to Cu stress, supporting our belief that *ribD* is not a false positive from our genetic screen. Nevertheless, future work to dissect the contribution of the *rib* locus to Cu stress resistance is now warranted.

Establishing a new collection of genes that confer GBS resistance to Cu stress expands our understanding of metal management in this organism and offers new insight into the genetic diversity mediating resistance to Cu intoxication in bacteria. For example, genes encoding enzymes for metabolism and cell wall synthesis, regulators, and transporters are critical for GBS to resist Cu stress. Four genes identified in the current study (*oafA, rfaB, plyB and yceG*) possess domains that are commonly found in proteins involved in cell wall biogenesis. Only mutation in *rfaB* (encoding a putative glycosyltransferase that may transfer sugar moieties to lipid, protein or carbohydrate residues) resulted in a reduction in cellular Cu content compared to WT during Cu stress. This finding leads us to present a model in which *rfaB* supports the central role of *copA* (12) in cellular Cu management in GBS. Based on Cu content data, the products of *plyB, oafA* and *yceG* do not contribute to cellular Cu status. As such, their exact contributions to

370 resisting Cu stress remains complex and requires further characterisation. It is
371 notable that in complementing our isogenic mutations, we could not successfully
372 obtain a clone of *oafA* using *E. coli* as a cloning host. Instead, we used chelation
373 as an approach to restore growth of our *oafA*-deficient strain during Cu stress.
374 Interestingly, we also note that *in trans* complementation with *plyB* further
375 abrogated growth in Cu stress, suggesting that multiple copies of plasmid-borne
376 *plyB* may have a detrimental effect on GBS growth. Future studies characterizing
377 the exact functions of the *rfaB*, *plyB*, *yceG* and *oafA* genes will help to elucidate
378 mechanistic roles such as in restricting Cu import, or compensating for pathways
379 that are susceptible to Cu poisoning. Such work will yield new understanding of
380 the cellular processes that underpin bacterial resistance to Cu intoxication.
381
382 Bacterial resistance to metal stress is a fitness trait of some pathogens that is
383 used to evade host defence responses (35, 36), and several studies have shown
384 that Cu management contributes to bacterial pathogenicity. For example, *S.*
385 *pneumoniae* regulates central metabolism in response to metal stress to support
386 its survival (17), and uses CopA for virulence during infection (10). In *E. coli*, Cu-
387 transporting ATPases, including CopA are required for survival in macrophages
388 (37). We recently demonstrated that *copA* contributes to the ability for GBS to
389 colonize and survive in the mammalian host during acute infection (12).
390 Together, these studies and the results of the current work show that Cu
391 management is an important facet of various bacterial pathogens, including GBS
392 in their ability to infect a host. Other observations of bacterial pathogens support

393 a role for Cu management in bacterial virulence in host niches. For example,
394 increased expression of *copY* in *S. pneumoniae* in the lungs of mice was
395 reported (10), and higher Cu levels along with co-incidental up-regulation of
396 *copYAZ* in the blood of mice infected with *S. pyogenes* was reported (11).
397 Characterization of the contributions of the genes of the Cu resistome identified
398 in this current study to GBS virulence will be important to explore potential roles
399 in pathogenesis.
400
401 Overall, our application of a highly saturated mutant library combined with deep
402 sequencing provides valuable insight into the Cu stress resistome of GBS. Our
403 study identifies a unique collection of genetic targets (including *hisMJP*, *oafA*,
404 *yceG*, *plyB*, *ribD*, *rfaB* and *stp1*) that are new to the field of metal detoxification in
405 bacteria and it will be of interest to study their effects towards resistance to metal
406 stress in other pathogens. Together, these findings provide new insight into the
407 repertoire of mechanisms used by GBS to survive Cu stress, and which may be
408 relevant to other bacteria.
409

Materials and Methods

Bacterial strains, plasmids and growth conditions

GBS, *E. coli* and plasmids used are listed in Supplementary Table S3. GBS was routinely grown in Todd-Hewitt Broth (THB) or on TH agar (1.5% w/v). *E. coli* was grown in Lysogeny Broth (LB) or on LB agar. Routine retrospective colony counts were performed by plating dilutions of bacteria on tryptone soya agar containing 5% defibrinated horse blood (Thermo Fisher Scientific). Media were supplemented with antibiotics (spectinomycin (Sp) 100µg/mL), as indicated. Growth assays used 200µL culture volumes in 96-well plates (Greiner) sealed using Breathe-Easy® membranes (Sigma-Aldrich) and measured attenuance (D, at 600nm) using a ClarioSTAR multimode plate reader (BMG Labtech) in Well Scan mode using a 3mm 5x5 scan matrix with 5 flashes per scan point and path length correction of 5.88mm, with agitation at 300rpm and recordings taken every 30min. Media for growth assays were THB, a modified Chemically-Defined Medium (CDM) (24) (with 1g/L glucose, 0.11g/L pyruvate and 50mg/L L-cysteine),supplemented with Cu (supplied as $CuSO_4$) and/or TPEN (N,N,N′,N′-Tetrakis(2-pyridylmethyl)ethylenediamine; Sigma-Aldrich) as indicated. For attenuance baseline correction, control wells without bacteria were included for Cu in media alone.

DNA extraction and genetic modification of GBS

Plasmid DNA was isolated using miniprep kits (QIAGEN), with modifications for GBS as described elsewhere (38). All strains and primers used are listed in Supplementary Tables S3 and S4 respectively. Mutant strains were constructed

via markerless allelic exchange using sequences (Supplementary Table S5) first synthesized in pUC57 (GenScript, USA) and subcloned into pHY304aad9 as previously described (24). Complement constructs were made by cloning the respective genes into shuttle vector pDL278. Mutants and complement constructs were validated by PCR using primers external to the mutation/cloning site and DNA sequencing.

Whole bacterial cell metal content determination

Metal content in cells was determined as described (39). Cultures were prepared essentially as described (12); THB medium was supplemented with 0.5 mM Cu or not supplemented (Ctrl), and following exposure for 2.5h, bacteria were harvested by centrifugation at 4122 x g at 4°C. Cell pellets were washed 3 times in PBS + 5mM EDTA to remove extracellular metals, followed by 3 washes in PBS. Pelleted cells were dried overnight at 80°C and resuspended in 1mL of 32.5% nitric acid and incubated at 95°C for 1h. The metal ion containing supernatant was collected by centrifugation (14,000 x g, 30min) and diluted to a final concentration of 3.25% nitric acid for metal content determination using inductively coupled plasma optical emission spectroscopy (ICP-OES). ICP-OES was carried out on an Agilent 720 ICP-OES with axial torch, OneNeb concentric nebulizer and Agilent single pass glass cyclone spray chamber. The power was 1.4kW with 0.75L/min nebulizer gas, 15L/min plasma gas and 1.5L/min auxiliary gas flow. Cu was analysed at 324.75nm, Zn at 213.85nm, Fe at 259.94nm and Mn at 257.61nm with detection limits at <1.1ppm. The final quantity of each metal was normalised using dry weight biomass of the cell pellet prior to nitric acid

digestion, expressed as $\mu g.g^{-1}$dry weight. Scandium was used as an internal standard for quality control in recovery in the ICP-OES analyses; recovery was >97% for all samples.

Transposon Directed Insertion Site Sequencing (TraDIS)

Generation and screening of the 874391:IS*S1* library was performed essentially as previously described (40), with some modifications. Briefly, the pGh9:IS*S1* plasmid (33) (provided by A. Charbonneau *et al*.) was transformed into WT GBS, and successful transformants were selected by growth on THB agar supplemented with 0.5µg/mL Erythromycin (Em). A single colony was picked and grown in 10mL of THB with 0.5µg/mL Em at 28°C overnight. The overnight cultures were incubated at 40°C for 3h to facilitate random transposition of IS*S1* into the bacterial chromosome. Transposon mutants were selected by plating cultures onto THB agar supplemented with Em and growing overnight at 37°C. Pools of the transposon mutants were harvested with a sterile spreader and stored in THB supplemented with 25% glycerol at -80°C. The final library of approximately 480,000 mutants was generated by pooling two independent batches of mutants.

Exposure of the library used approximately 1.9×10^8 bacteria inoculated into 100mL of THB (non-exposed control) or THB supplemented with 1.5 mM Cu in THB. The cultures were grown for 12 h at 37°C (shaking), and subsequently, 10mL of culture were removed and washed once with PBS. Genomic DNA was extracted from three cell pellets per condition (prepared as independent biological samples) using the DNeasy UltraClean Microbial Kit (Qiagen)

according to the manufacturer's instructions, except that the cell pellets were incubated with 100 units of mutanolysin and 40mg of RNase A at 37°C for 90min. Genomic DNA was subjected to library preparation as previously described (29), with slight modifications. Briefly, the NEBNext dsDNA fragmentase (New England BioLabs) was used to generate DNA fragments in the range of 200-800bp. An in-house Y-adapter was generated by mixing and incubating adaptor primers 1 and 2 for 2min at 95°C, and chilling the reaction to 20°C by incremental decreases in temperature by 0.1°C. The reaction was placed on ice for 5min, and ice cold ultra-pure water was added to dilute the reaction to 15µM. The Y-adaptor was ligated to the ends of the fragments using the NEBNext Ultra II DNA Library Prep Kit for Illumina (New England BioLabs) according to the manufacturer's instructions. All adaptor ligated fragments were incubated with *Not*I.HF (New England BioLabs) for 2h at 37°C to deplete plasmid fragments. The digested fragments were PCR amplified as per the protocol outlined in the NEBNext Ultra II DNA Library Prep Kit using a specific IS*S1* primer and reverse indexing primer. DNA quantification was undertaken using a QuBit dsDNA HS Assay Kit (Invitrogen) and purified using AMPure XP magnetic beads (Beckman Coulter). All libraries were pooled and submitted for sequencing on the MiSeq platform at the Australian Centre for Ecogenomics (University of Queensland, Australia). The sequencing data generated from TraDIS libraries were analysed used the Bio-TraDIS scripts (41) on raw demultiplexed sequencing reads. Reads containing the transposon tag (CAGAAAACTTTGCAACAGAACC) were filtered and mapped to the genome of WT GBS 874391 using the bacteria_tradis script

with the “--smalt_y 1” and “--smalt_r 0” parameters to ensure accuracy of insertion mapping. Subsequent analysis steps to determine log_2 fold-change (log_2FC), false discovery rate (FDR) and P value were carried out with the AlbaTraDIS script (42). To identify genes in 874391 required for resistance to Cu intoxication condition used, we used a stringent criteria of log_2FC ≤ -2 or ≥ 2, FDR <0.001 and P value <0.05. The TraDIS reads are deposited in the Sequence Read Archive (SRA) under BioProject ID: PRJNA674399.

Statistical methods

All statistical analyses used GraphPad Prism V8 and are defined in respective Figure Legends. Statistical significance was accepted at P values of ≤0.05.

Acknowledgments

We gratefully acknowledge Andrew Waller and Amy Charbonneau, Animal Health Trust (Suffolk, UK) for providing pGh9-IS*S1*. We thank Michael Crowley and David Crossman of the Heflin Center for Genomic Science Core Laboratories, University of Alabama at Birmingham (Birmingham, AL) for RNA sequencing. We also thank Lahiru Katupitiya and Dean Gosling for excellent technical assistance. This work was supported by a Project Grant from the National Health and Medical Research Council (NHMRC) Australia (APP1146820 to GCU).

Table 1. Genes identified in TraDIS screen as significantly under-represented and over-represented.

Locus tag[#]	Gene	Annotation	log_2FC	log_{10}CPM
01047	*hisM**	amino acid ABC transporter permease	-6.41	7.63
01048	*hisJ**	amino acid ABC transporter ATP-binding protein	-6.37	7.37
01049	*hisP**	amino acid ABC transporter substrate-binding protein	-4.94	7.98
00507	*copA*	Cu-translocating P-type ATPase	-3.98	9.27
00084	*oafA**	acyltransferase	-3.80	11.04
00083	-	membrane protein	-3.78	9.02
01646	*yceG**	MltG-like endolytic transglycosylase	-3.64	5.80
00435	*stp1**	Stp1/IreP family PP2C-type Ser/Thr phosphatase	-2.10	5.96
00288	*ackA*	acetate kinase	2.04	7.22
00879	*ribH*	6 and 7-dimethyl-8-ribityllumazine synthase	2.40	7.98
00877	*ribE*	riboflavin synthase	2.46	8.12
00876	*ribD**	bifunctional diamino-hydroxyphospho-ribosyl-amino-pyrimidine deaminase/5-amino-6-(5-phosphoribosylamino) uracil reductase RibD	2.67	9.19
00878	*ribA*	bifunctional 3 and 4-dihydroxy-2-butanone-4-phosphate synthase/GTP cyclohydrolase II	2.74	9.00

[#]Denotes GBS str 874391 locus tag, preceded by CHF17_; * denotes genes that were mutated for this study

Figure 1. Growth of WT GBS 874391 and a *copA*-deficient mutant in Cu stress. The bacteria were grown in THB supplemented with 1.5 mM Cu for 12 h. Points show means of attenuance (D, 600nm) and bars show s.e.m. (*n*=3).

Figure 2. Defining the Cu resistome of GBS using TraDIS. (A) Experimental design to identify genes associated with Cu stress. A super-saturated GBS IS*S1* library is inoculated into THB (Ctrl) or THB + 1.5 mM Cu (+Cu) and grown for 12 h to stationary phase. Bacterial genomic DNA is then extracted and subjected to sequencing and TraDIS analysis. (B) TraDIS analysis of the GBS Cu resistome identified 5 genes that were significantly over-represented (blue), and 8 genes that were significantly under-represented (red), using highly stringent cut-offs ($2 \leq \log_2FC \leq -2$; FDR < 0.001 and P value < 0.05). A further 28 and 15 were significantly under- or over-represented between 2-4-fold ($\log_2$ FC $\pm$1-2), respectively. Horizontal dashed lines highlight FC cutoffs of $2 \leq \log_2FC \leq -2$ and solid lines indicate cutoffs of $1 \leq \log_2FC \leq -1$.

Figure 3. Insertion plots of genes associated with Cu resistance as identified by TraDIS. Individual insertions mapped to the *copYAZ* (A), *hisMJP* (B), *oafA* (C), *stp1* (D), *yceG* (E) and *ribDEAH* (F) loci are shown, with vertical dotted lines denoting the boundaries of each genetic element. The number of reads mapped per bp are shown in the non-exposed control in grey and the Cu-

549 stress condition in blue. Genes without annotation are identified by the GBS
550 strain 874391 locus tag numbers that are preceded by CHF17_0 (e.g.
551 CHF17_01645).

552

553 **Figure 4**. **Viability analysis of isogenic mutant strains that contribute to**
554 **resistance to Cu stress in THB media**. Colony forming unit (CFU) assays of
555 WT GBS and isogenic mutants grown in THB or THB + 1.5mM Cu for 12 h. P
556 values calculated with independent *t*-tests comparing THB and THB + 1.5 mM Cu
557 (***, P < 0.001; **, P < 0.01; *, P < 0.05; ns = not significant) Data are means of 3
558 independent repeats with error bars indicating SD.

559

560 **Figure 5**. **Growth kinetics of GBS and isogenic mutants in THB medium**
561 **with and without Cu stress**. (A) Growth curves of GBS and derivative mutants
562 in THB + 1.5 mM Cu (Cu stress; blue lines) compared to THB alone (control;
563 black lines). Data are compiled from measurements of attenuance (D; 600nm)
564 every 30 minutes with solid lines as means and shaded area indicating s.e.m
565 from ≥ 3 independent experiments. Cu stress data for each strain was compared
566 to control data using area under the curve (A.U.C) analysis followed by
567 independent *t*-tests with significance indicated at the top right of each panel. The
568 growth kinetics of the WT strain were compared to each of the isogenic mutant

strains using AUC and independent *t*-tests in THB (B; control, black) and in THB + 1.5 mM Cu (C; Cu stress, blue) (*P<0.05, **P<0.01,***P<0.005)

Figure 6. **Growth kinetics of GBS and isogenic mutants in CDM medium with and without Cu stress**. (A) Growth curves of GBS and derivative mutants in CDM + 0.5 mM Cu (Cu stress; blue lines) compared to CDM alone (control; black lines). Data are compiled from measurements of attenuance (D; 600nm) every 30 minutes with solid lines as means and shaded area indicating s.e.m from ≥ 3 independent experiments. Cu stress data for each strain was compared to control data using area under the curve (A.U.C) analysis followed by independent *t*-tests with significance indicated at the top right of each panel. The growth kinetics of the WT strain were compared to each of the isogenic mutant strains using AUC and independent *t*-tests in CDM (B; control, black) and in CDM + 0.5 mM Cu (C; Cu stress, blue) (*P<0.05, **P<0.01,***P<0.005).

Figure 7. Intracellular Cu content in WT GBS 874391 and isogenic mutants in Cu stress. (A) Total intracellular Cu content was compared in WT and isogenic mutants grown in THB with and without supplemental Cu (0.5 mM) and normalised using dry weight biomass (μg Cu per mg). (B) Ratio of intracellular Cu content in isogenic mutants compared to WT in Cu stress. Data presented are means of 3 independent repeats with error bars indicating standard deviation and

590 compared by independent *t*-tests (ns = not significant, * P < 0.05, ** P < 0.01, ***
591 P < 0.005).
592
593

References

1. Osman D, Cavet JS. 2008. Copper homeostasis in bacteria. Adv Appl Microbiol 65:217-47.
2. Djoko KY, Goytia MM, Donnelly PS, Schembri MA, Shafer WM, McEwan AG. 2015. Copper(II)-Bis(Thiosemicarbazonato) Complexes as Antibacterial Agents: Insights into Their Mode of Action and Potential as Therapeutics. Antimicrob Agents Chemother 59:6444-53.
3. Achard Maud ES, Stafford Sian L, Bokil Nilesh J, Chartres J, Bernhardt Paul V, Schembri Mark A, Sweet Matthew J, McEwan Alastair G. 2012. Copper redistribution in murine macrophages in response to *Salmonella* infection. Biochem J 444:51-57.
4. Djoko KY, Ong CL, Walker MJ, McEwan AG. 2015. The Role of Copper and Zinc Toxicity in Innate Immune Defense against Bacterial Pathogens. J Biol Chem 290:18954-61.
5. Chandrangsu P, Rensing C, Helmann JD. 2017. Metal homeostasis and resistance in bacteria. Nature Reviews Microbiology 15:338-350.
6. German N, Doyscher D, Rensing C. 2013. Bacterial killing in macrophages and amoeba: do they all use a brass dagger? Future Microbiol 8:1257-64.
7. Besold AN, Culbertson EM, Culotta VC. 2016. The Yin and Yang of copper during infection. Journal of Biological and Inorganic Chemistry 21:137-44.

8. Ladomersky E, Petris MJ. 2015. Copper tolerance and virulence in bacteria. Metallomics 7:957-64.

9. O'Brien H, Alvin JW, Menghani SV, Sanchez-Rosario Y, Van Doorslaer K, Johnson MDL. 2020. Rules of Expansion: an Updated Consensus Operator Site for the CopR-CopY Family of Bacterial Copper Exporter System Repressors. mSphere 5.

10. Shafeeq S, Yesilkaya H, Kloosterman TG, Narayanan G, Wandel M, Andrew PW, Kuipers OP, Morrissey JA. 2011. The *cop* operon is required for copper homeostasis and contributes to virulence in *Streptococcus pneumoniae*. Mol Microbiol 81:1255-70.

11. Stewart LJ, Ong CY, Zhang MM, Brouwer S, McIntyre L, Davies MR, Walker MJ, McEwan AG, Waldron KJ, Djoko KY. 2020. Role of Glutathione in Buffering Excess Intracellular Copper in *Streptococcus pyogenes*. mBio 11.

12. Sullivan MJ, Goh KG, Gosling D, Katupitiya L, Ulett GC. 2021. Copper intoxication in group B Streptococcus triggers transcriptional activation of the *cop* operon that contributes to enhanced virulence during acute infection. J Bacteriol in press.

13. Edwards MS, Baker CJ. 2018. 119 - *Streptococcus agalactiae* (Group B *Streptococcus*), p 723-729.e1. *In* Long SS, Prober CG, Fischer M (ed), Principles and Practice of Pediatric Infectious Diseases (Fifth Edition) doi:https://doi.org/10.1016/B978-0-323-40181-4.00119-5. Elsevier.

638 14. Lindahl G, Stalhammar-Carlemalm M, Areschoug T. 2005. Surface
639 proteins of *Streptococcus agalactiae* and related proteins in other bacterial
640 pathogens. Clin Microbiol Rev 18:102-27.
641 15. Festa RA, Thiele DJ. 2011. Copper: an essential metal in biology. Curr
642 Biol 21:R877-83.
643 16. Hodgkinson V, Petris MJ. 2012. Copper homeostasis at the host-pathogen
644 interface. J Biol Chem 287:13549-55.
645 17. Burcham LR, Hill RA, Caulkins RC, Emerson JP, Nanduri B, Rosch JW,
646 Fitzkee NC, Thornton JA. 2020. *Streptococcus pneumoniae* metal
647 homeostasis alters cellular metabolism. Metallomics 12:1416-1427.
648 18. Hooven TA, Catomeris AJ, Bonakdar M, Tallon LJ, Santana-Cruz I, Ott S,
649 Daugherty SC, Tettelin H, Ratner AJ. 2018. The *Streptococcus agalactiae*
650 Stringent Response Enhances Virulence and Persistence in Human
651 Blood. Infect Immun 86.
652 19. Zhu L, Yerramilli P, Pruitt L, Saavedra MO, Cantu CC, Olsen RJ, Beres
653 SB, Waller AS, Musser JM. 2020. Genome-wide assessment of
654 *Streptococcus agalactiae* genes required for fitness in human whole blood
655 and plasma. Infect Immun doi:10.1128/IAI.00357-20.
656 20. Burnside K, Lembo A, Harrell MI, Gurney M, Xue L, BinhTran NT,
657 Connelly JE, Jewell KA, Schmidt BZ, de los Reyes M, Tao WA, Doran KS,
658 Rajagopal L. 2011. Serine/threonine phosphatase Stp1 mediates post-
659 transcriptional regulation of hemolysin, autolysis, and virulence of group B
660 Streptococcus. J Biol Chem 286:44197-210.

21. Rajagopal L, Vo A, Silvestroni A, Rubens CE. 2006. Regulation of cytotoxin expression by converging eukaryotic-type and two-component signalling mechanisms in *Streptococcus agalactiae*. Mol Microbiol 62:941-57.

22. Lin WJ, Walthers D, Connelly JE, Burnside K, Jewell KA, Kenney LJ, Rajagopal L. 2009. Threonine phosphorylation prevents promoter DNA binding of the Group B Streptococcus response regulator CovR. Mol Microbiol 71:1477-95.

23. Rajagopal L, Clancy A, Rubens CE. 2003. A eukaryotic type serine/threonine kinase and phosphatase in *Streptococcus agalactiae* reversibly phosphorylate an inorganic pyrophosphatase and affect growth, cell segregation, and virulence. J Biol Chem 278:14429-41.

24. Sullivan MJ, Goh KGK, Ulett GC. 2021. Cellular Management of Zinc in Group B Streptococcus Supports Bacterial Resistance against Metal Intoxication and Promotes Disseminated Infection. mSphere 6.

25. Johnson MD, Kehl-Fie TE, Rosch JW. 2015. Copper intoxication inhibits aerobic nucleotide synthesis in *Streptococcus pneumoniae*. Metallomics 7:786-94.

26. Rajagopal L, Vo A, Silvestroni A, Rubens CE. 2005. Regulation of purine biosynthesis by a eukaryotic-type kinase in *Streptococcus agalactiae*. Mol Microbiol 56:1329-46.

27. Tarrant E, G PR, McIlvin MR, Stevenson J, Barwinska-Sendra A, Stewart LJ, Saito MA, Waldron KJ. 2019. Copper stress in Staphylococcus aureus

684 leads to adaptive changes in central carbon metabolism. Metallomics
685 11:183-200.
686 28. Kelley LA, Mezulis S, Yates CM, Wass MN, Sternberg MJ. 2015. The
687 Phyre2 web portal for protein modeling, prediction and analysis. Nature
688 Protoccols 10:845-58.
689 29. Rubino JT, Franz KJ. 2012. Coordination chemistry of copper proteins:
690 how nature handles a toxic cargo for essential function. J Inorg Biochem
691 107:129-43.
692 30. Kothary V, Doster RS, Rogers LM, Kirk LA, Boyd KL, Romano-Keeler J,
693 Haley KP, Manning SD, Aronoff DM, Gaddy JA. 2017. Group B
694 Streptococcus Induces Neutrophil Recruitment to Gestational Tissues and
695 Elaboration of Extracellular Traps and Nutritional Immunity. Frontiers in
696 Cellular and Infection Microbiology 7:19.
697 31. Samen U, Gottschalk B, Eikmanns BJ, Reinscheid DJ. 2004. Relevance of
698 peptide uptake systems to the physiology and virulence of *Streptococcus*
699 *agalactiae*. J Bacteriol 186:1398-408.
700 32. Deschamps P, Kulkarni PP, Gautam-Basak M, Sarkar B. 2005. The saga
701 of copper(II)–l-histidine. Coordination Chemistry Reviews 249:895-909.
702 33. Maguin E, Prevost H, Ehrlich SD, Gruss A. 1996. Efficient insertional
703 mutagenesis in lactococci and other gram-positive bacteria. J Bacteriol
704 178:931-5.
705 34. Baker J, Sitthisak S, Sengupta M, Johnson M, Jayaswal RK, Morrissey
706 JA. 2010. Copper stress induces a global stress response in

Staphylococcus aureus and represses sae and agr expression and biofilm formation. Appl Environ Microbiol 76:150-60.

35. Kapetanovic R, Bokil NJ, Achard ME, Ong CL, Peters KM, Stocks CJ, Phan MD, Monteleone M, Schroder K, Irvine KM, Saunders BM, Walker MJ, Stacey KJ, McEwan AG, Schembri MA, Sweet MJ. 2016. *Salmonella* employs multiple mechanisms to subvert the TLR-inducible zinc-mediated antimicrobial response of human macrophages. FASEB J 30:1901-12.

36. Stocks CJ, Phan MD, Achard MES, Nhu NTK, Condon ND, Gawthorne JA, Lo AW, Peters KM, McEwan AG, Kapetanovic R, Schembri MA, Sweet MJ. 2019. Uropathogenic *Escherichia coli* employs both evasion and resistance to subvert innate immune-mediated zinc toxicity for dissemination. Proc Natl Acad Sci U S A 116:6341-6350.

37. White C, Lee J, Kambe T, Fritsche K, Petris MJ. 2009. A role for the ATP7A copper-transporting ATPase in macrophage bactericidal activity. J Biol Chem 284:33949-56.

38. Sullivan MJ, Ulett GC. 2018. Stable Expression of Modified Green Fluorescent Protein in Group B Streptococci To Enable Visualization in Experimental Systems. Appl Environ Microbiol 84.

39. Eijkelkamp BA, Morey JR, Ween MP, Ong CL, McEwan AG, Paton JC, McDevitt CA. 2014. Extracellular zinc competitively inhibits manganese uptake and compromises oxidative stress management in *Streptococcus pneumoniae*. PLoS ONE 9:e89427.

729 40. Charbonneau ARL, Forman OP, Cain AK, Newland G, Robinson C,
730 Boursnell M, Parkhill J, Leigh JA, Maskell DJ, Waller AS. 2017. Defining
731 the ABC of gene essentiality in streptococci. BMC Genomics 18:426.
732 41. Barquist L, Mayho M, Cummins C, Cain AK, Boinett CJ, Page AJ,
733 Langridge GC, Quail MA, Keane JA, Parkhill J. 2016. The TraDIS toolkit:
734 sequencing and analysis for dense transposon mutant libraries.
735 Bioinformatics 32:1109-11.
736 42. Page AJ, Bastkowski S, Yasir M, Turner AK, Le Viet T, Savva GM,
737 Webber MA, Charles IG. 2020. AlbaTraDIS: Comparative analysis of large
738 datasets from parallel transposon mutagenesis experiments. PLoS
739 Comput Biol 16:e1007980.
740

Figure 1.

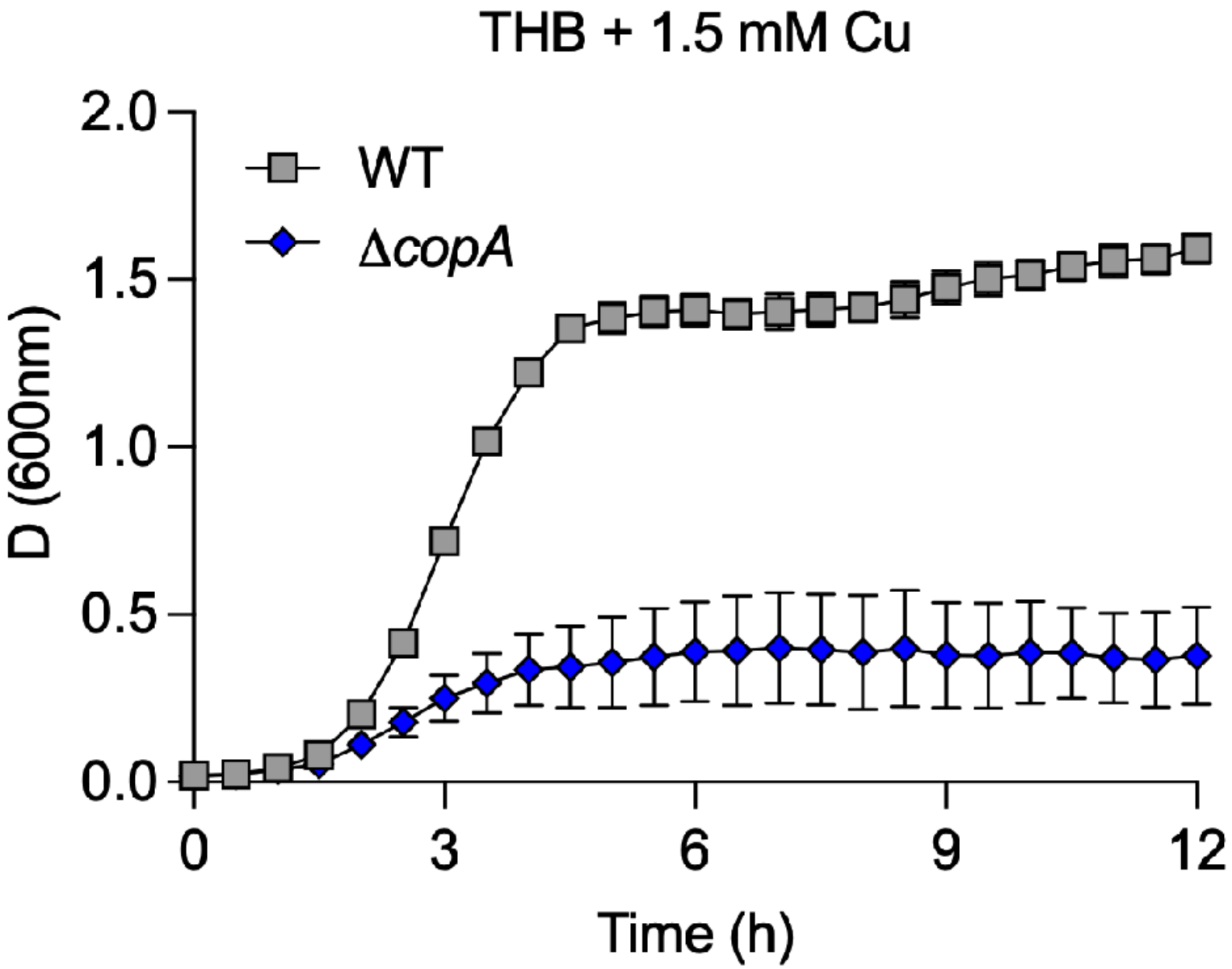

Figure 2

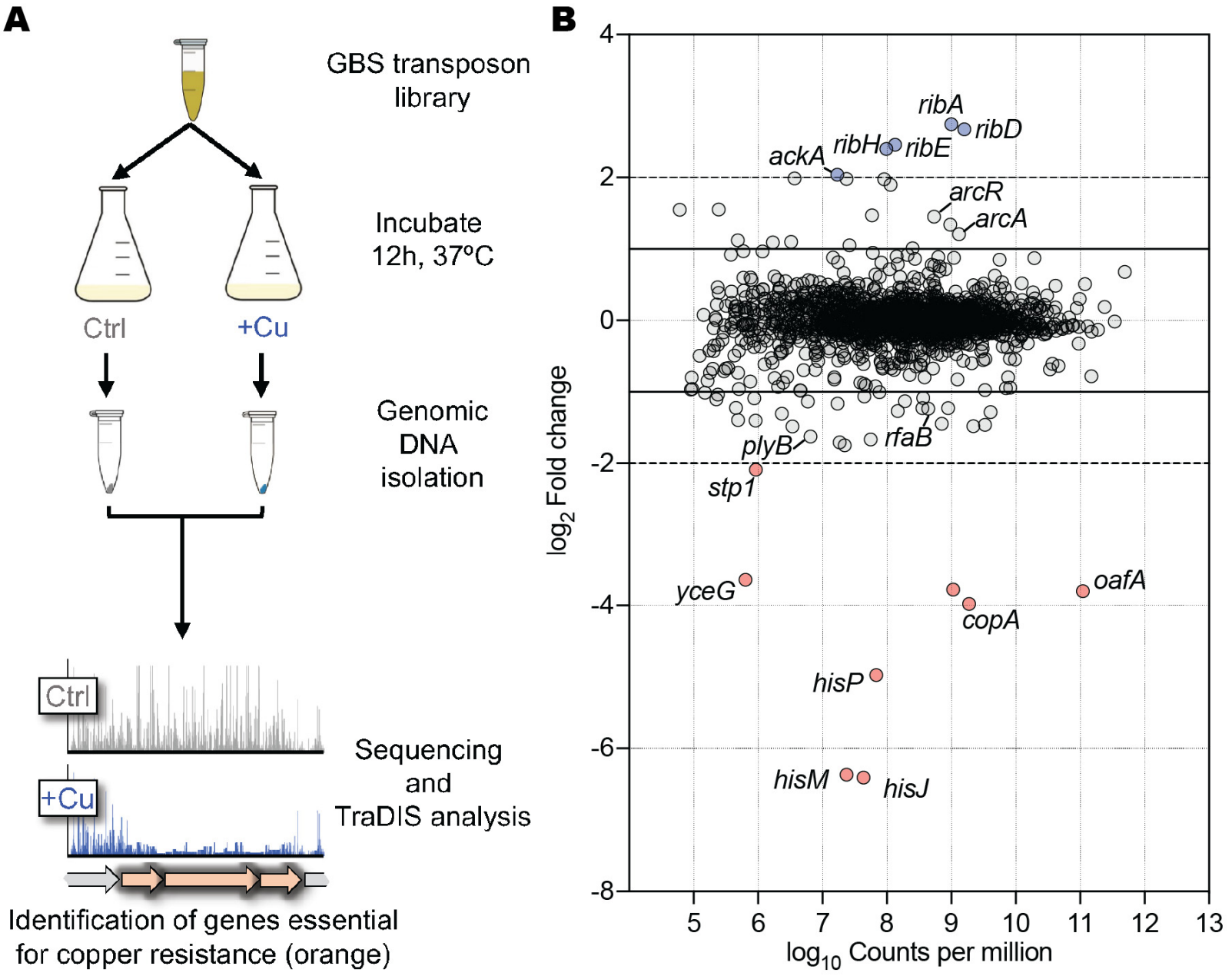
A
GBS transposon library
Incubate 12h, 37°C
Ctrl
+Cu
Genomic DNA isolation
Ctrl
+Cu
Sequencing and TraDIS analysis
Identification of genes essential for copper resistance (orange)
B
log2 Fold change
log10 Counts per million
ribA
ribD
ribH
ribE
ackA
arcR
arcA
rfaB
plyB
stp1
yceG
copA
oafA
hisP
hisM
hisJ

Figure 3

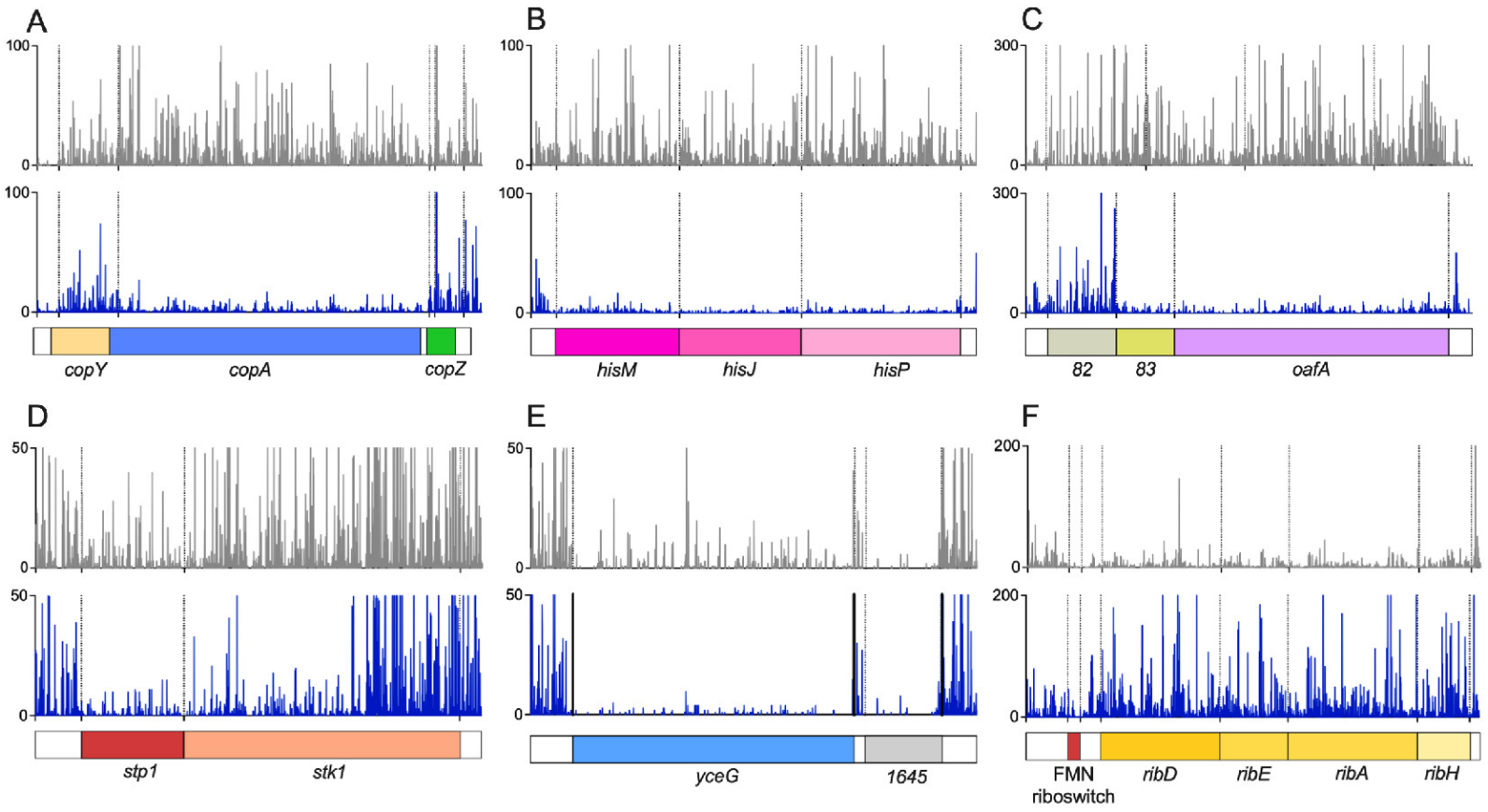
A
100
0
100
0
copY
copA
copZ
B
100
0
100
0
hisM
hisJ
hisP
C
300
0
300
0
82
83
oafA
D
50
0
50
0
stp1
stk1
E
50
0
50
0
yceG
1645
F
200
0
200
0
FMN
riboswitch
ribD
ribE
ribA
ribH

Figure 4

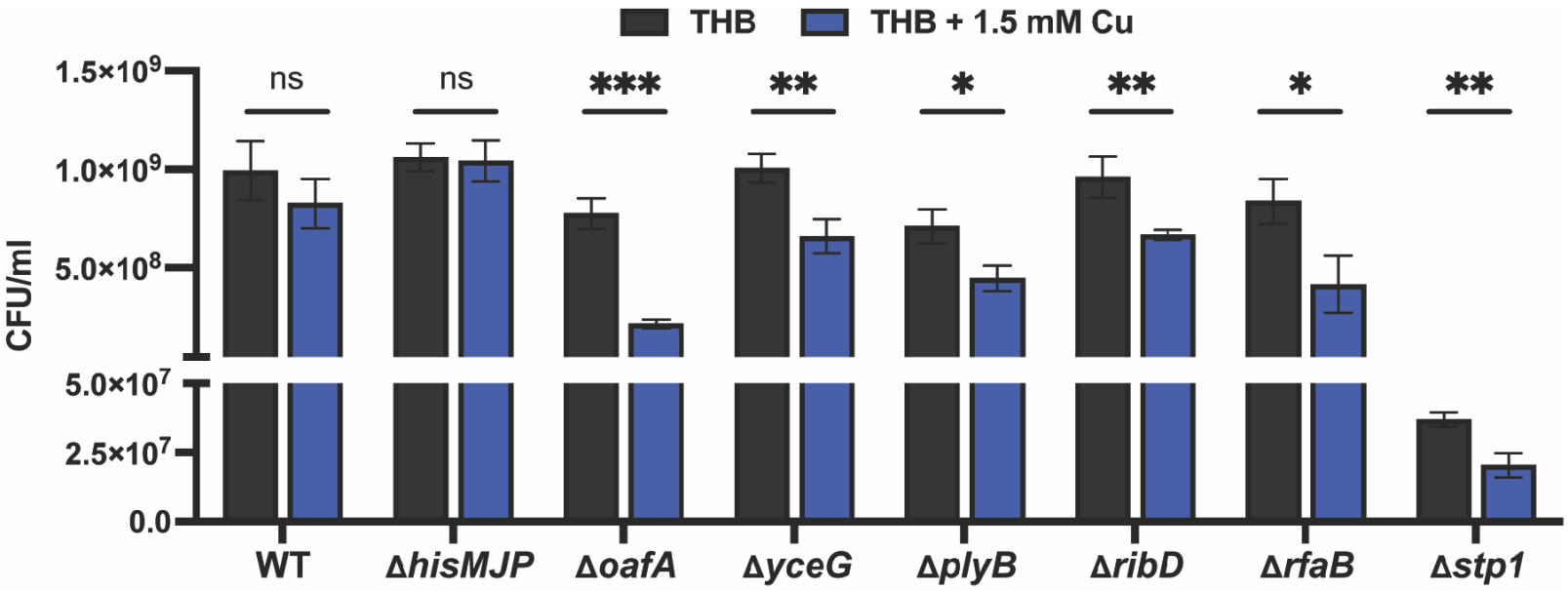
THB
THB + 1.5 mM Cu
CFU/ml
1.5×10^9
1.0×10^9
5.0×10^8
5.0×10^7
2.5×10^7
0.0
ns
ns
***
**
*
**
*
**
WT
ΔhisMJP
ΔoafA
ΔyceG
ΔplyB
ΔribD
ΔrfaB
Δstp1

Figure 5

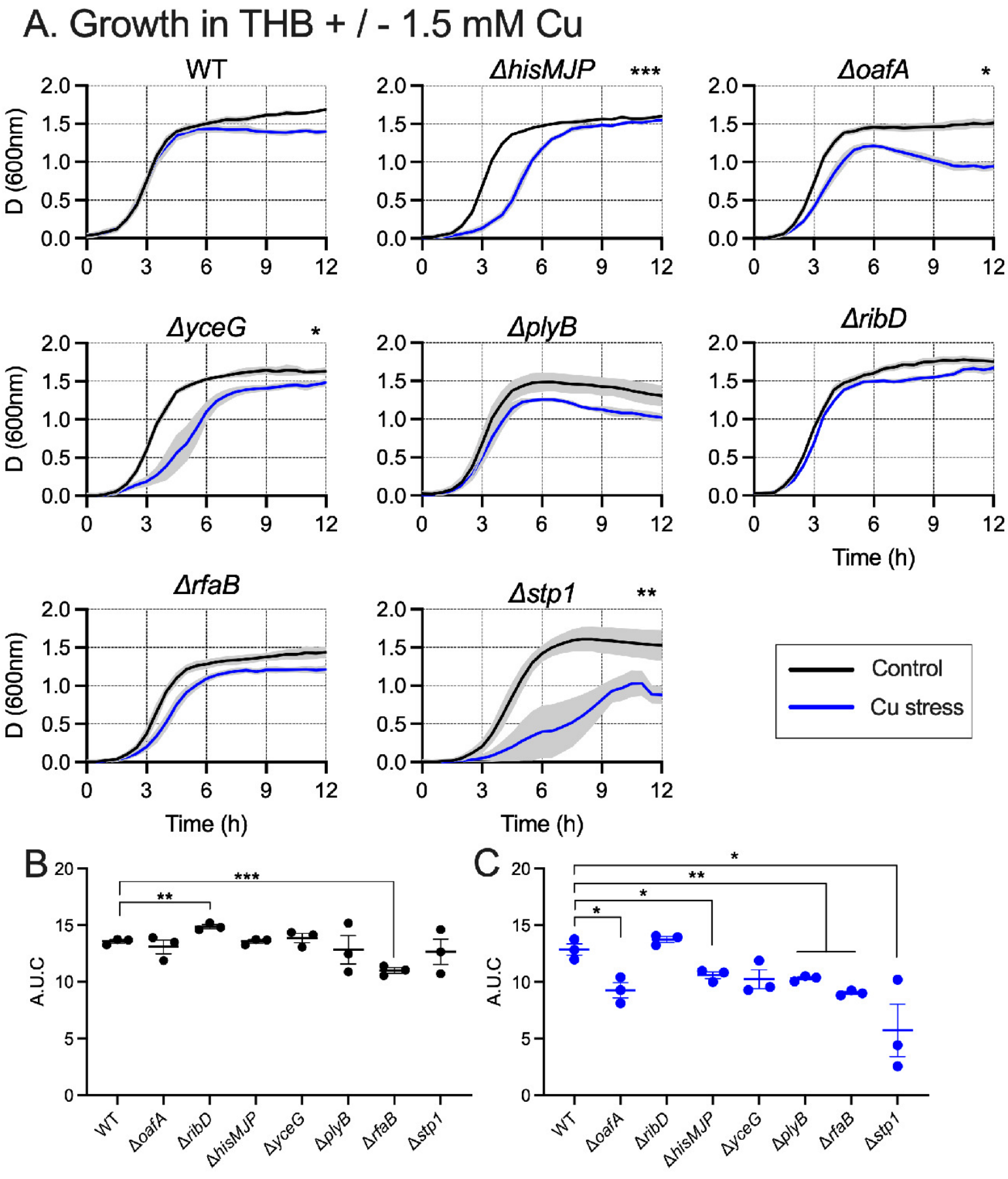
A. Growth in THB + / - 1.5 mM Cu
WT
ΔhisMJP
***
ΔoafA
*
ΔyceG
*
ΔplyB
ΔribD
ΔrfaB
Δstp1
**
D (600nm)
Time (h)
Control
Cu stress
B
C
A.U.C
WT
ΔoafA
ΔribD
ΔhisMJP
ΔyceG
ΔplyB
ΔrfaB
Δstp1

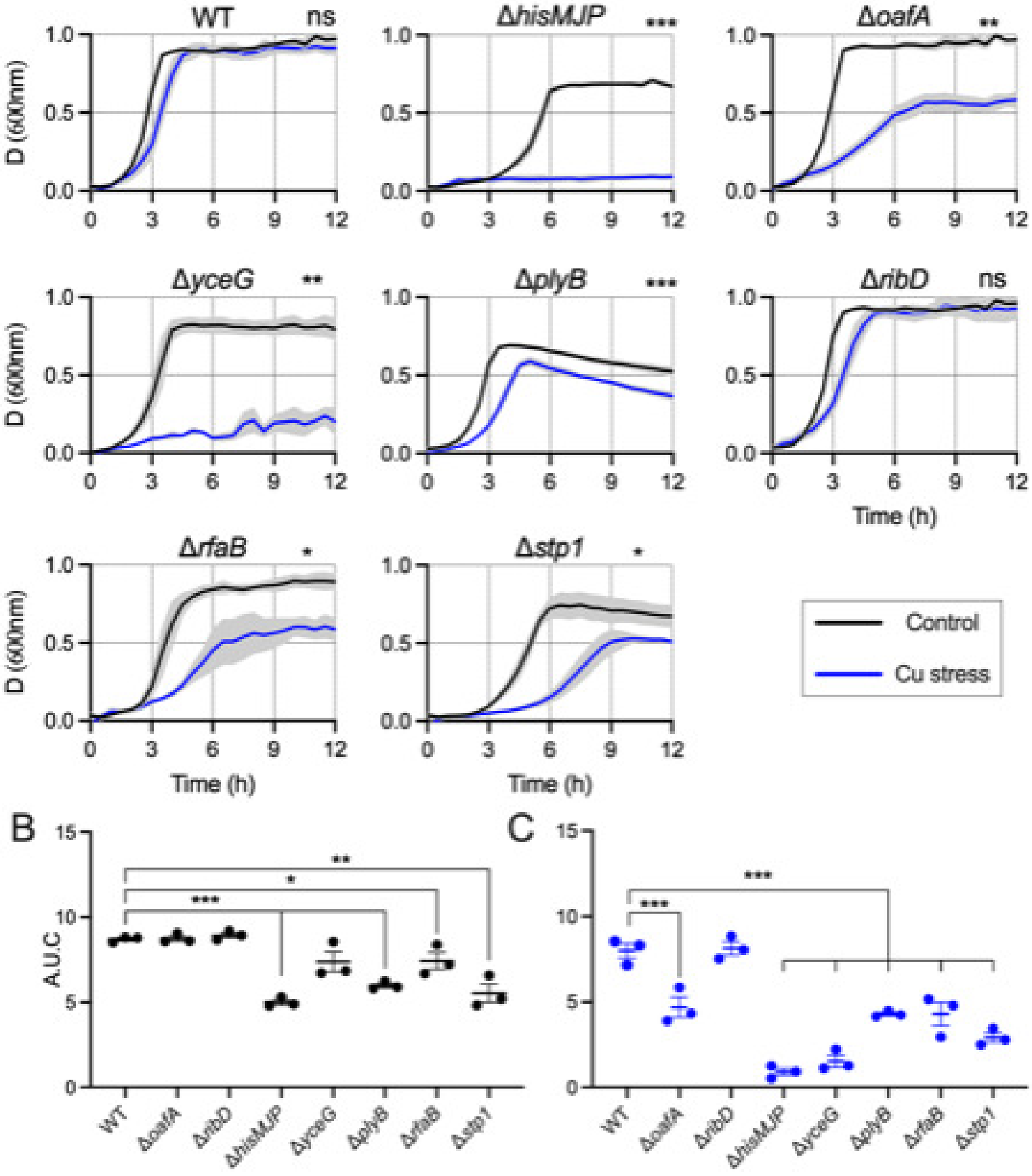
A. Growth in CDM + / - 0.5 mM Cu
WT
ns
ΔhisMJP
***
ΔoafA
**
ΔyceG
**
ΔplyB
***
ΔribD
ns
ΔrfaB
*
Δstp1
*
D (600nm)
Time (h)
Control
Cu stress
B
C
A.U.C
WT
ΔoafA
ΔribD
ΔhisMJP
ΔyceG
ΔplyB
ΔrfaB
Δstp1

Figure 7

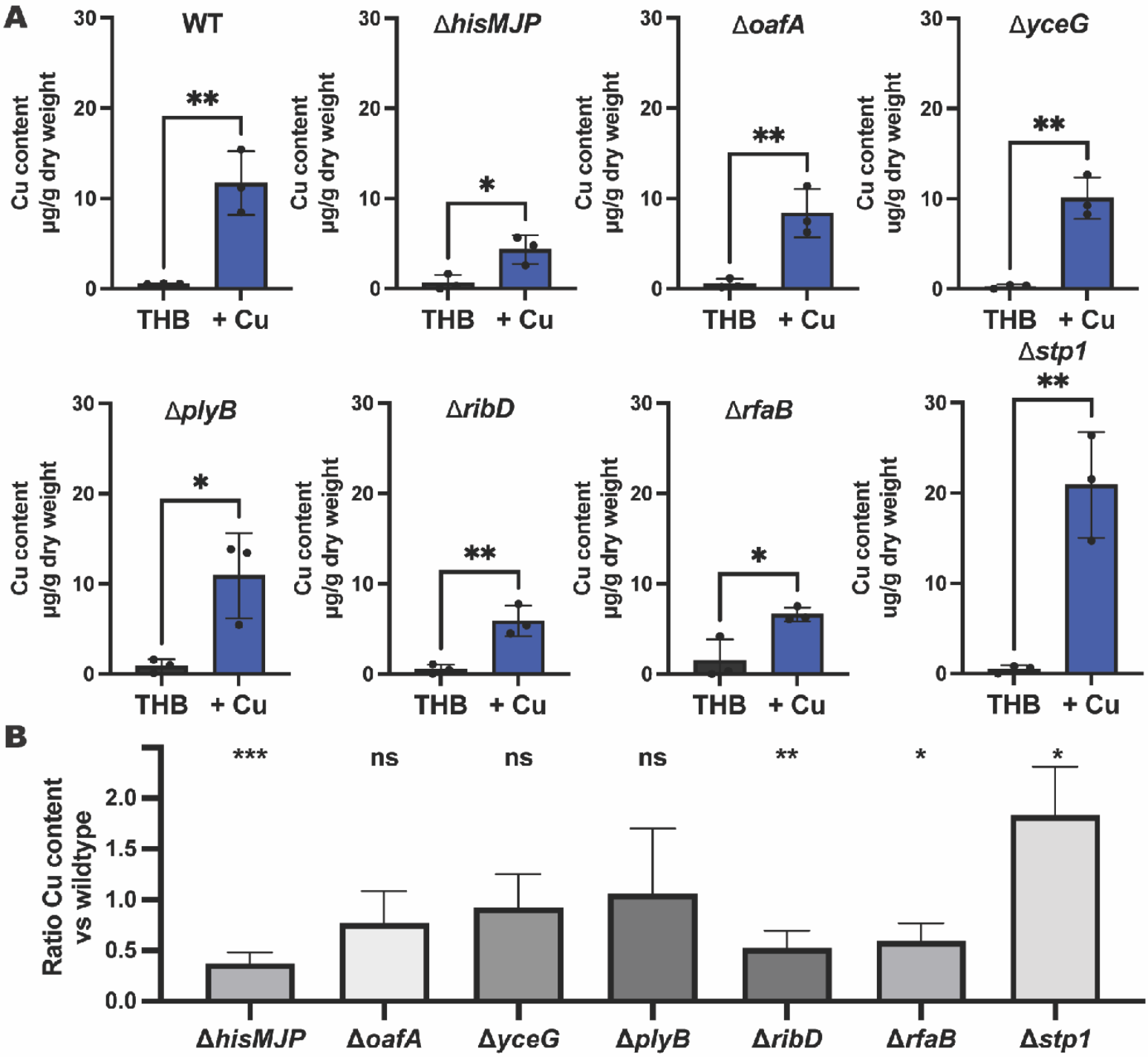
A
WT
ΔhisMJP
ΔoafA
ΔyceG
ΔplyB
ΔribD
ΔrfaB
Δstp1
Cu content µg/g dry weight
THB
+ Cu
B
Ratio Cu content vs wildtype
ΔhisMJP
ΔoafA
ΔyceG
ΔplyB
ΔribD
ΔrfaB
Δstp1
***
ns
ns
ns
**
*
*